Liquid Crystals
Publication details, including instructions for authors and subscription information:
http://www.informaworld.com/smpp/title~content=t713926090

Circularly polarized fluorescence from chiral nematic liquid crystalline films: theory and experiment

Hongqin Shi; Brooke M. Conger; Dimitris Katsis; Shaw H. Chen

Online publication date: 06 August 2010

To cite this Article Shi, Hongqin , Conger, Brooke M. , Katsis, Dimitris and Chen, Shaw H.(1998) 'Circularly polarized fluorescence from chiral nematic liquid crystalline films: theory and experiment', Liquid Crystals, 24: 2, 163 — 172
To link to this Article: DOI: 10.1080/026782998207334
URL: http://dx.doi.org/10.1080/026782998207334

LIQUID CRYSTALS, 1998, VOL. 24, NO. 2, 163–172

Circularly polarized fluorescence from chiral nematic liquid crystalline films: theory and experiment

by HONGQIN SHI, BROOKE M. CONGER, DIMITRIS KATSIS and SHAW H. CHEN*

Materials Science Program, Chemical Engineering Department and Laboratory for Laser Energetics, Center for Optoelectronics and Imaging, University of Rochester, 240 E. River Road, Rochester, NY 14623-1212, USA

(*Received 29 October 1996; in final form 5 April 1997; accepted 8 April 1997*)

A theory was formulated for the description of circularly polarized fluorescence (CPF) from a chiral nematic film in the spectral region outside the selective reflection band. The CPF theory incorporates: (1) the ability of a chiral nematic film to accomplish both circular dichroism and circular polarization and (2) linearly polarized fluorescence from chromophores unaxially aligned in the nematic sublayers comprising the film. Chiral nematic fluid films consisting of a nematic fluid, BDH 18523, and a chiral dopant, cholesteryl oleate, were prepared for hosting 1,6-diphenylhexatriene as a fluorescent dye. The experimentally determined dissymmetry factor using both left- and right-handed circularly polarized excitations was found to be in good agreement with the theoretical prediction with all the system parameters determined *a priori*. The theory was also employed to furnish insight into the effects of the concentration of the fluorescent dye and chiral nematic film thickness on the dissymmetry factor.

1. Introduction

Cholesteric mesomorphism can be generated by mixing a nematic liquid crystal with a chiral compound. The molecules spontaneously assemble themselves into a helical stack of nematic layers with the helical axis perpendicular to the substrates. If a fluorescent chromophore is molecularly dispersed into such a chiral nematic film, the long axis of the dopant molecules will align with the nematic director in each layer, resulting in circular dichroism (CD) [1] and circularly polarized fluorescence (CPF) [2]. The degree of CPF is expressed by the dissymmetry factor, g_e, defined as

$$g_e = 2\frac{I_L - I_R}{I_L + I_R} \tag{1}$$

where I_L and I_R are the intensity of the left- and right-handed CPF, respectively. Stegemeyer *et al.* [2], Pollmann *et al.* [3], and Sisido *et al.* [4], found that the absolute value of g_e can be as high as 0·3 using chiral nematic fluid films.

Pollmann *et al.* [3], proposed a theory of CPF based on de Vries' theory of light propagation in a chiral nematic film. Specifically, their theory was developed for the range of fluorescence wavelengths, λ_F, far shorter than the selective reflection wavelength, λ_R, namely,

$$\lambda_F^* = \frac{\lambda_F}{\lambda_R} \ll 1. \tag{2}$$

In this wavelength range, they treated two limiting cases, $\lambda_F^* \gg n^*$ and $\lambda_F^* \ll n^*$, where $n^* = 2(n_\xi - n_\eta)/(n_\xi + n_\eta)$ is the relative birefringence of the nematic sublayer with its director parallel and perpendicular to the ξ- and η-axis, respectively. In addition, absorption was considered to occur isotropically, which is equivalent to ignoring CD of the excitation beam. The theory was employed to account for experimental observations under the stated limiting conditions [2] and to furnish insight into the structure of excimers [4–6].

In the general theory to be presented below, the spectral region outside of selective reflection is considered without restrictions imposed by Pollmann *et al.* [3]. Moreover, both CD and film thickness are properly accounted for. Relevant experimental results are also presented to validate the theory.

2. Theory

A chiral nematic LC film is known to be capable of circular polarization (CP) of an unpolarized light source. Various theories have been formulated, and the one presented recently by Good and Karali [7] was adopted in this study for the description of CP by a chiral

*Author for correspondence.

nematic film. To facilitate development of a theory of CPF, let us begin with the wave equations for light propagation along the helical axis, z:

$$\frac{\partial^2 E_x}{\partial z^2} = \frac{1}{c^2}\left(\varepsilon_{xx}\frac{\partial^2 E_x}{\partial t^2} + \varepsilon_{xy}\frac{\partial^2 E_y}{\partial t^2}\right)$$

and (3)

$$\frac{\partial^2 E_y}{\partial z^2} = \frac{1}{c^2}\left(\varepsilon_{xy}\frac{\partial^2 E_x}{\partial t^2} + \varepsilon_{yy}\frac{\partial^2 E_y}{\partial t^2}\right)$$

where c is the speed of light in a vacuum and ε_{ij}s are the elements in the dielectric tensor:

$$\varepsilon_{xx} = \varepsilon(1 + \delta\cos 2\theta), \qquad \varepsilon_{yy} = \varepsilon(1 - \delta\cos 2\theta),$$
$$\varepsilon_{xy} = \varepsilon_{yx} = \varepsilon\delta\sin 2\theta, \qquad \varepsilon = \frac{1}{2}(\varepsilon_\xi + \varepsilon_\eta),$$
$$\delta = \frac{\varepsilon_\xi - \varepsilon_\eta}{\varepsilon_\xi + \varepsilon_\eta}, \qquad \theta = qz, \tag{4}$$
$$q = 2\pi/p, \qquad p = \frac{\lambda_R}{\varepsilon^{1/2}}.$$

In equations (3) and (4), E and ε are the electric component of the light wave and dielectric constant, respectively, and p is the helical pitch length of the cholesteric host with a positive value for a right-handed helix and negative for a left-handed helix. In a low optical birefringence environment, $p = \lambda_R/\varepsilon^{1/2}$, since $\varepsilon^{1/2} \cong n$, the average index of refraction. Equation (3) can be solved more conveniently in terms of the circular components, E^+ and E^-:

$$E^{\pm} = \sum_{j=1}^{4} E_j^{\pm} = \sum_{j=1}^{4} A_j^{\pm} e^{i(l_j \pm 1)qz}\, e^{-i\omega t} = E_x \pm iE_y \tag{5}$$

where

$$l_j = \pm[1 + \lambda^{*-2} \pm (4\lambda^{*-2} + \lambda^{*-4}\delta^2)^{1/2}]^{1/2}$$
$$(l_1^2 > l_2^2 \text{ and } l_3 = -l_1,\ l_4 = -l_2),$$
$$\frac{A_j^+}{A_j^-} = \frac{\delta}{(l_j+1)^2\lambda^{*2} - 1} = \frac{(l_j-1)^2\lambda^{*2} - 1}{\delta}, \qquad \lambda^* = \frac{\lambda}{\lambda_R}, \tag{6}$$

and λ is the wavelength , i.e. $\lambda = \lambda_F$ or λ_{ex}, the excitation wavelength. Note that E^+ and E^- represent the right- and left-handed circular component, respectively, for light propagating in the positive z-direction. For light propagating in the negative z-direction, E^+ and E^- represent the left- and right-handed circular component, respectively. With continuity of both the electric and magnetic fields at film surfaces serving as boundary conditions, coefficients $A_j^{\pm}$ in equation (5) were determined. In the following, $\mathbf{E}$ is used to represent the electric field in the circular space, and $\bar{\mathbf{E}}$ the electric field in the linear space.

$$\mathbf{E} = \begin{pmatrix} E^+ \\ E^- \end{pmatrix}, \qquad \bar{\mathbf{E}} = \begin{pmatrix} E_\xi \\ E_\eta \end{pmatrix}. \tag{7}$$

The chiral nematic film is depicted in figure 1 for implementation of equation (5) in a problem in which fluorescence from within the film is treated. It is assumed that there is no reabsorption of the emitted light in the absence of an overlap between the absorption and the emission spectra. A CPF film is envisioned to consist of a large number of emissive nematic sublayers, with an arbitrary one being located at $z = -b$. As depicted in figure 2, the photo-excited emission process involving this arbitrary layer occurs via the following mechanism: (1) the excitation beam enters the film at $z = -\tau$ and propagates in the positive z-direction; (2) both anisotropic absorption and circular polarization of the excitation beam occur as it propagates through the film before reaching $z = -b$; (3) absorption by chromophores at $z = -b$ leads to linearly polarized emission; (4) part of the fluorescent beam propagates from $z = -b$ in the positive z-direction, while being circularly polarized, and is detected at $z = 0$. With an objective of calculating g_e of the transmitted beam as detected at $z = 0$, the theory is developed as follows.

2.1. *Excitation at* z = −b

An excitation beam of any polarization state at $z = -\tau$ can be written in terms of circularly polarized components:

$$\boldsymbol{E}_{-\tau}^{ex} = \begin{pmatrix} E_\tau^{ex+} \\ E_\tau^{ex-} \end{pmatrix} = \begin{pmatrix} E_{in}^{ex+} \\ E_{in}^{ex-} \end{pmatrix} e^{ik_1(z+\tau) - i\omega_f t} \tag{8}$$

where $E_{-\tau}^{ex+}$ and $E_{-\tau}^{ex-}$ represent the incident right- and

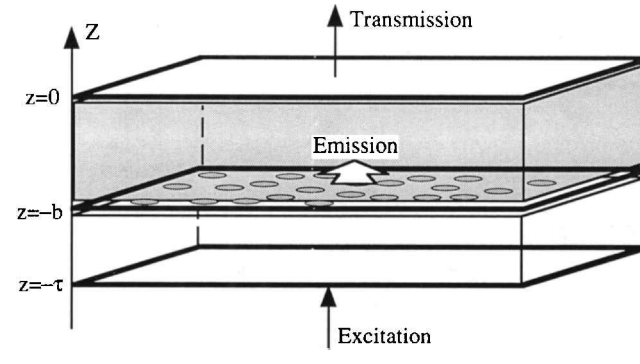

Figure 1. A schematic of a chiral nematic film with a thickness τ capable of photo-excited emission from within the film. For an emissive nematic layer at $z = -b$, a sub-film of thickness b serves to accomplish circular polarization of the fluorescent beam.

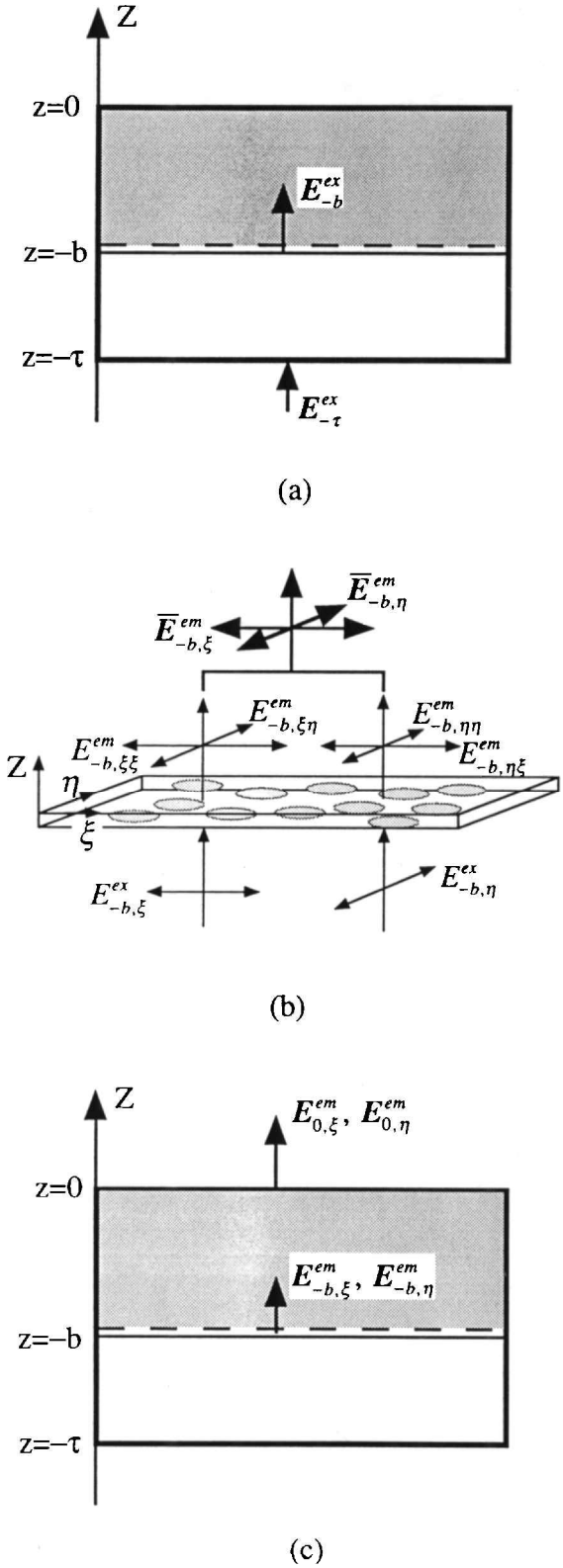

Figure 2. The underlying optical processes of CPF from within a chiral nematic film: (*a*) Excitation beam propagates from $z=-\tau$ to $z=-b$ while undergoing CD and CP. (*b*) Absorption of $\boldsymbol{E}^{\mathrm{ex}}_{-b}$ by chromophores in a nematic layer at $z=-b$ results in two linearly polarized fluorescent beams, $\bar{\boldsymbol{E}}^{\mathrm{em}}_{-b,\xi}$ and $\bar{\boldsymbol{E}}^{\mathrm{em}}_{-b,\eta}$. (*c*) Fluorescent beam propagates from $z=-b$ to $z=0$ while undergoing CP.

left-handed circularly polarized components at $z=-\tau$, and $k_1=2\pi n/\lambda_{\mathrm{ex}}$, in which n is the average index of the nematic sublayer. Upon travelling from $z=-\tau$ to $z=-b$, the incident excitation $\boldsymbol{E}^{\mathrm{ex}}_{-\tau}$ is circularly polarized into $\boldsymbol{E}^{\mathrm{ex}}_{-b}$, according to Good and Karali's theory [7]:

$$\boldsymbol{E}^{\mathrm{ex}}_{-b}=\boldsymbol{T}(\tau-b)\ \boldsymbol{E}^{\mathrm{ex}}_{-\tau} \tag{9}$$

where the transmission matrix, $\boldsymbol{T}$, is expressed below:

$$\boldsymbol{T}(\tau-b)=\boldsymbol{T}(\zeta)|_{\zeta=\tau-b}=\begin{pmatrix} T_{11} & T_{12} \\ T_{21} & T_{22} \end{pmatrix} \tag{10}$$

with

$$\begin{aligned} T_{11}&=a_{23}A_{11}+a_{24}A_{12}+a_{21}A_{13}+a_{22}A_{14},\\ T_{12}&=a_{23}A_{21}+a_{24}A_{22}+a_{21}A_{23}+a_{22}A_{24},\\ T_{21}&=a_{13}A_{11}+a_{14}A_{12}+a_{11}A_{13}+a_{12}A_{14},\\ T_{22}&=a_{13}A_{21}+a_{14}A_{22}+a_{11}A_{23}+a_{12}A_{24}, \end{aligned} \tag{11}$$

$$A_{11}=\frac{1}{D}\begin{vmatrix} a_{12} & a_{13} & a_{14} \\ a_{22} & a_{23} & a_{24} \\ a_{42} & a_{43} & a_{44} \end{vmatrix},\qquad A_{12}=-\frac{1}{D}\begin{vmatrix} a_{11} & a_{13} & a_{14} \\ a_{21} & a_{23} & a_{24} \\ a_{41} & a_{43} & a_{44} \end{vmatrix},$$

$$A_{13}=\frac{1}{D}\begin{vmatrix} a_{11} & a_{12} & a_{14} \\ a_{21} & a_{22} & a_{24} \\ a_{41} & a_{42} & a_{44} \end{vmatrix},\qquad A_{14}=-\frac{1}{D}\begin{vmatrix} a_{11} & a_{12} & a_{13} \\ a_{21} & a_{22} & a_{23} \\ a_{41} & a_{42} & a_{43} \end{vmatrix},$$

$$A_{21}=-\frac{1}{D}\begin{vmatrix} a_{12} & a_{13} & a_{14} \\ a_{22} & a_{23} & a_{24} \\ a_{32} & a_{33} & a_{34} \end{vmatrix},\qquad A_{22}=\frac{1}{D}\begin{vmatrix} a_{11} & a_{13} & a_{14} \\ a_{21} & a_{23} & a_{24} \\ a_{31} & a_{33} & a_{34} \end{vmatrix},$$

$$A_{23}=-\frac{1}{D}\begin{vmatrix} a_{11} & a_{12} & a_{14} \\ a_{21} & a_{22} & a_{24} \\ a_{31} & a_{32} & a_{34} \end{vmatrix},\qquad A_{24}=\frac{1}{D}\begin{vmatrix} a_{11} & a_{12} & a_{13} \\ a_{21} & a_{22} & a_{23} \\ a_{31} & a_{32} & a_{33} \end{vmatrix}, \tag{12}$$

$$D=\begin{vmatrix} a_{11} & a_{12} & a_{13} & a_{14} \\ a_{21} & a_{22} & a_{23} & a_{24} \\ a_{31} & a_{32} & a_{33} & a_{34} \\ a_{41} & a_{42} & a_{43} & a_{44} \end{vmatrix}, \tag{13}$$

$$
\begin{aligned}
a_{11}(\zeta) &= (1-\rho_1)(1-\beta-\beta l_1),\\
a_{12}(\zeta) &= (1-\rho_2)(1-\beta-\beta l_2),\\
a_{13}(\zeta) &= (1+\rho_1)(1-\beta+\beta l_1),\\
a_{14}(\zeta) &= (1+\rho_2)(1-\beta+\beta l_2),\\
a_{21}(\zeta) &= (1+\rho_1)(1+\beta-\beta l_1),\\
a_{22}(\zeta) &= (1+\rho_2)(1+\beta-\beta l_2),\\
a_{23}(\zeta) &= (1-\rho_1)(1+\beta+\beta l_1),\\
a_{24}(\zeta) &= (1-\rho_1)(1+\beta+\beta l_2),\\
a_{31}(\zeta) &= (1-\rho_1)(1+\beta+\beta l_1)\,\mathrm{e}^{-\mathrm{i}l_1 q\zeta},\\
a_{32}(\zeta) &= (1-\rho_2)(1+\beta+\beta l_2)\,\mathrm{e}^{-\mathrm{i}l_2 q\zeta},\\
a_{33}(\zeta) &= (1+\rho_1)(1+\beta-\beta l_1)\,\mathrm{e}^{\mathrm{i}l_1 q\zeta},\\
a_{34}(\zeta) &= (1+\rho_2)(1+\beta-\beta l_2)\,\mathrm{e}^{\mathrm{i}l_2 q\zeta},\\
a_{41}(\zeta) &= (1+\rho_1)(1-\beta+\beta l_1)\,\mathrm{e}^{-\mathrm{i}l_1 q\zeta},\\
a_{42}(\zeta) &= (1+\rho_2)(1-\beta+\beta l_2)\,\mathrm{e}^{-\mathrm{i}l_2 q\zeta},\\
\mathrm{a}_{43}(\zeta) &= (1-\rho_1)(1-\beta-\beta \mathrm{l}_1)\,\mathrm{e}^{\mathrm{i}l_1 q\zeta},\\
a_{44}(\zeta) &= (1-\rho_2)(1-\beta-\beta l_2)\,\mathrm{e}^{\mathrm{i}l_2 q\zeta},
\end{aligned}
\tag{14}
$$

$$
\rho_j = \frac{1 - A_j^{+}/A_j^{-}}{1 + A_j^{+}/A_j^{-}} (j = 1, 2, 3, 4), \qquad \beta = \lambda_{\mathrm{F}}^{*} \text{ or } \lambda_{\mathrm{ex}}^{*}.
\tag{15}
$$

Because of the boundary conditions imposed by Good and Karali [7], the elements contained in $\boldsymbol{T}$ are applicable to a low optical birefringence host, such as BDH 18523 mixed with cholesteryl oleate employed in the present work (§3).

Besides CP, the excitation beam is attenuated via CD as it propagates through the film. To account for both CP and CD in the calculation of $\boldsymbol{E}_{-b}^{\mathrm{ex}}$ using equation (9), dielectric constants ε, ε_ξ and ε_η in equation (4) should be replaced by their complex counterparts, ε', ε'_ξ and ε'_η [8]:

$$
\varepsilon' = (n')^2 = (n + \mathrm{i}\kappa)^2, \qquad \varepsilon'_\xi = (n'_\xi)^2 = (n_\xi + \mathrm{i}\kappa_\xi)^2,
$$

and

$$
\varepsilon'_\eta = (n'_\eta)^2 = (n_\eta + \mathrm{i}\kappa_\eta)^2.
\tag{16}
$$

Note that the real part, n, is responsible for CP, whereas the imaginary part, κ, known as the extinction index, is for CD. Moreover, extinction indices κ, κ_ξ and κ_η are related to molar extinction coefficients α, α_ξ and α_η through equation (17):

$$
\kappa = \frac{2{\cdot}303\,\alpha C \lambda_{\mathrm{ex}}}{4\pi}, \qquad \kappa_\xi = \frac{2{\cdot}303\,\alpha_\xi C \lambda_{\mathrm{ex}}}{4\pi},
$$

and

$$
\kappa_\eta = \frac{2{\cdot}303\,\alpha_\eta C \lambda_{\mathrm{ex}}}{4\pi}
\tag{17}
$$

where C is the molar concentration of chromophore, and

$$
\alpha_\xi = \alpha(1 + 2S_{\mathrm{ab}}) \qquad \text{and} \qquad \alpha_\eta = \alpha(1 - S_{\mathrm{ab}})
\tag{18}
$$

in which S_{ab} is the second-rank order parameter related to anisotropic absorption, and α the average molar extinction coefficient. The above equations are applicable to a chiral nematic film consisting of fluorescent molecules. In the case of a fluorescent dye doped into a chiral nematic host, which does not absorb or emit light, molecular ordering and anisotropic absorption both refer to guest molecules.

The parameters directly relevant to the description of fluorescence are the intensities of excitation at $z = -b$, $I_{-b,\xi}^{\mathrm{ex}}$ and $I_{-b,\eta}^{\mathrm{ex}}$ as evaluated by equation (19):

$$
I_{-b,\xi}^{\mathrm{ex}} \propto |E_{-b,\xi}^{\mathrm{ex}}|^2 \qquad \text{and} \qquad I_{-b,\eta}^{\mathrm{ex}} \propto |E_{-b,\eta}^{\mathrm{ex}}|^2
\tag{19}
$$

where $E_{-b,\xi}^{\mathrm{ex}}$ and $E_{-b,\eta}^{\mathrm{ex}}$ are the linearly polarized components of excitation, which can be calculated from the circularly polarized components $E_{-b}^{\mathrm{ex}+}$ and $E_{-b}^{\mathrm{ex}-}$ given by equation (9) with complex refractive indices:

$$
\begin{aligned}
\bar{\boldsymbol{E}}_{-b}^{\mathrm{ex}} &= \begin{pmatrix} E_{-b,\xi}^{\mathrm{ex}} \\ E_{-b,\eta}^{\mathrm{ex}} \end{pmatrix} = 0{\cdot}5 \begin{pmatrix} \mathrm{e}^{\mathrm{i}qb} & \mathrm{e}^{-\mathrm{i}qb} \\ -\mathrm{i}\mathrm{e}^{\mathrm{i}qb} & \mathrm{i}\mathrm{e}^{-\mathrm{i}qb} \end{pmatrix} \begin{pmatrix} E_{-b}^{\mathrm{ex}+} \\ E_{-b}^{\mathrm{ex}} \end{pmatrix} \\
&= 0{\cdot}5 \begin{pmatrix} \mathrm{e}^{\mathrm{i}qb} & \mathrm{e}^{-\mathrm{i}qb} \\ -\mathrm{i}\mathrm{e}^{\mathrm{i}qb} & \mathrm{i}\mathrm{e}^{-\mathrm{i}qb} \end{pmatrix} \boldsymbol{E}_{-b}^{\mathrm{ex}}.
\end{aligned}
\tag{20}
$$

Note that equation (19) is characterized by two proportionality constants [9], $n_\xi/2\eta_0$ and $n_\eta/2\eta_0$, where η_0 is the impedance of free space, and n_ξ and n_η are the indices of refraction of the local nematic sublayer along the long and short molecular axis, respectively. It is evident that for a relatively low optical birefringence liquid crystal host, the two proportionality constants should be practically identical. Consequently, the single proportionality constant characterizing the two intensities, $I_{-b,\xi}^{\mathrm{ex}}$ and $I_{-b,\eta}^{\mathrm{ex}}$, will eventually cancel itself in the calculation of g_{e} using equation (1).

2.2. *Fluorescence at* z = − b

The fluorescence intensity at $z = -b$ is proportional to the magnitude of the absorption and emission transition moments squared, $|\bar{\boldsymbol{M}}_{\mathrm{a}}|^2$ and $|\bar{\boldsymbol{M}}_{\mathrm{e}}|^2$, and the excitation intensity in an isotropic environment [10]. This general relationship is extended in this study for the treatment of emission from a uniaxially aligned nematic sublayer. With respect to the long molecular axis, the absorption transition moment normally makes a negligibly small angle, whereas the emission transition moment is characterized by an angle φ. When the molecules at $z = -b$ are excited by linearly polarized light $E_{-b,\xi}^{\mathrm{ex}}$ and $E_{-b,\eta}^{\mathrm{ex}}$, representing the waves along the ξ- and η-axis, respectively, the emitted wave at $z = -b$,

can be expressed in terms of two incoherent waves according to the theory of linearly polarized fluorescence (LPF) [11]:

$$\bar{\boldsymbol{E}}^{\mathrm{em}}_{-b,\xi}=\begin{pmatrix} E^{\mathrm{em}}_{-b,\xi} \\ 0 \end{pmatrix}; \qquad \bar{\boldsymbol{E}}^{\mathrm{em}}_{-b,\eta}=\begin{pmatrix} 0 \\ E^{\mathrm{em}}_{-b,\eta} \end{pmatrix} \tag{21}$$

where

$$E^{\mathrm{em}}_{-b,\xi} \propto \sqrt{(I^{\mathrm{em}}_{-b,\xi\xi}+I^{\mathrm{em}}_{-b,\eta\xi})}\, \mathrm{e}^{\mathrm{i}k_1(z+b)-\mathrm{i}\omega_2 t} \tag{22}$$

and

$$E^{\mathrm{em}}_{-b,\eta} \propto \sqrt{(I^{\mathrm{em}}_{-b,\xi\eta}+I^{\mathrm{em}}_{-b,\eta\eta})}\, \mathrm{e}^{\mathrm{i}k_2(z+b)-\mathrm{i}\omega_2 t} \tag{23}$$

with

$$I^{\mathrm{em}}_{-b,\xi\xi}=\gamma_0 n_{\mathrm{a},\xi} n^3_{\mathrm{e},\xi} I^{\mathrm{ex}}_{-b,\xi} |\bar{\boldsymbol{M}}_{\mathrm{a}}|^2 |\bar{\boldsymbol{M}}_{\mathrm{e}}|^2 \times \left\{ \left(\frac{1}{5}+\frac{4}{7}S_{\mathrm{em}}+\frac{8}{35}\langle P_4\rangle_{\mathrm{em}} \right)\cos^2\varphi + \left(\frac{1}{15}+\frac{1}{21}S_{\mathrm{em}}-\frac{4}{35}\langle P_4\rangle_{\mathrm{em}} \right)\sin^2\varphi \right\} \tag{24}$$

$$I^{\mathrm{em}}_{-b,\xi\eta}=\gamma_0 n_{\mathrm{a},\xi} n^3_{\mathrm{e},\eta} I^{\mathrm{ex}}_{-b,\xi} |\bar{\boldsymbol{M}}_{\mathrm{a}}|^2 |\bar{\boldsymbol{M}}_{\mathrm{e}}|^2 \times \left\{ \left(\frac{1}{5}+\frac{1}{21}S_{\mathrm{em}}-\frac{4}{35}\langle P_4\rangle_{\mathrm{em}} \right)\cos^2\varphi + \left(\frac{2}{15}+\frac{13}{42}S_{\mathrm{em}}-\frac{2}{35}\langle P_4\rangle_{\mathrm{em}} \right)\sin^2\varphi \right\} \tag{25}$$

$$I^{\mathrm{em}}_{-b,\eta\xi}=\gamma_0 n_{\mathrm{a},\eta} n^3_{\mathrm{e},\xi} I^{\mathrm{ex}}_{-b,\eta} |\bar{\boldsymbol{M}}_{\mathrm{a}}|^2 |\bar{\boldsymbol{M}}_{\mathrm{e}}|^2 \times \left\{ \left(\frac{1}{15}+\frac{1}{21}S_{\mathrm{em}}-\frac{4}{35}\langle P_4\rangle_{\mathrm{em}} \right)\cos^2\varphi + \left(\frac{2}{15}+\frac{4}{21}S_{\mathrm{em}}+\frac{2}{35}\langle P_4\rangle_{\mathrm{em}} \right)\sin^2\varphi \right\} \tag{26}$$

$$I^{\mathrm{em}}_{-b,\eta\eta}=\gamma_0 n_{\mathrm{a},\eta} n^3_{\mathrm{e},\eta} I^{\mathrm{ex}}_{-\mathrm{b},\eta} |\bar{\boldsymbol{M}}_{\mathrm{a}}|^2 |\bar{\boldsymbol{M}}_{\mathrm{e}}|^2 \times \left\{ \left(\frac{1}{5}-\frac{2}{7}S_{\mathrm{em}}+\frac{3}{35}\langle P_4\rangle_{\mathrm{em}} \right)\cos^2\varphi + \left(\frac{1}{15}-\frac{1}{42}S_{\mathrm{em}}-\frac{3}{70}\langle P_4\rangle_{\mathrm{em}} \right)\sin^2\varphi \right\} \tag{27}$$

where, $E^{\mathrm{em}}_{-b,\xi}$ and $E^{\mathrm{em}}_{-b,\eta}$ represent the emitted waves along the ξ- and η-axis, respectively, $k_2=2\pi n/\lambda_{\mathrm{F}}$, S_{em} and $\langle \mathrm{P_4}\rangle_{\mathrm{em}}$ are the second- and fourth-rank order parameters responsible for LPF from a nematic sublayer, and $\gamma_0=KC\tau/\lambda_{\mathrm{a}}\lambda_{\mathrm{e}}^3$ in which K is a universal constant, τ the total lifetime of the excited state, λ_{a} and λ_{e} the absorption and emission wavelength, respectively. Note that $I^{\mathrm{ex}}_{-b,\xi}$ and $I^{\mathrm{ex}}_{-b,\eta}$ in equations (24)–(27) are available through equation (19). Furthermore, in a low optical birefringence environment with a small wavelength dispersion of refractive index between λ_{a} and λ_{e}, $n_{\mathrm{a}}\cong n_{\mathrm{e}}$ and both indices of refraction are also practically directionally independent. Under these conditions, the emitted intensity is proportional to the excitation intensity, the magnitudes of the two transition moments, and the orientation of the emission transition moment with respect to the long molecular axis with a proportionality constant that will drop out of the calculation of g_{e} using equation (1).

2.3. *Transmission of fluorescence at* z = 0

The polarization state of the photo-excited emission will be modified upon travelling from $z=-b$ to $z=0$ in accordance with Good and Karali's theory. With the assumption of no overlap between the absorption and emission spectra presented by the chromophore, reabsorption of emission is precluded as it propagates from $z=-b$ to $z=0$. To employ Good and Karali's theory, the linearly polarized components $E^{\mathrm{em}}_{-b,\xi}$ and $E^{\mathrm{em}}_{-b,\eta}$ in equations (22) and (23) are first converted into circularly polarized components $E^{\mathrm{em}\pm}_{-b,\xi}$ and $E^{\mathrm{em}\pm}_{-b,\eta}$:

$$\boldsymbol{E}^{\mathrm{em}}_{-b,\xi}=\begin{pmatrix} E^{\mathrm{em}+}_{-b,\xi} \\ E^{\mathrm{em}-}_{-b,\xi} \end{pmatrix} =\begin{pmatrix} 1 & \mathrm{i} \\ 1 & -\mathrm{i} \end{pmatrix}\begin{pmatrix} \cos(-bq) & -\sin(-bq) \\ \sin(-bq) & \cos(-bq) \end{pmatrix}\bar{\boldsymbol{E}}^{\mathrm{em}}_{-b,\xi} \tag{28}$$

and

$$\boldsymbol{E}^{\mathrm{em}}_{-b,\eta}=\begin{pmatrix} E^{\mathrm{em}+}_{-b,\eta} \\ E^{\mathrm{em}-}_{-b,\eta} \end{pmatrix} =\begin{pmatrix} 1 & \mathrm{i} \\ 1 & -\mathrm{i} \end{pmatrix}\begin{pmatrix} \cos(-bq) & -\sin(-bq) \\ \sin(-bq) & \cos(-bq) \end{pmatrix}\bar{\boldsymbol{E}}^{\mathrm{em}}_{-b,\eta}. \tag{29}$$

The fluorescence beam transmitted at $z=0$ can then be found in terms of $\boldsymbol{E}^{\mathrm{em}}_{0,\xi}$ and $\boldsymbol{E}^{\mathrm{em}}_{0,\eta}$ using

$$\boldsymbol{E}^{\mathrm{em}}_{0,\xi}=\begin{pmatrix} E^{\mathrm{em}+}_{0,\xi} \\ E^{\mathrm{em}-}_{0,\xi} \end{pmatrix}=\boldsymbol{T}(b)\ \ \boldsymbol{E}^{\mathrm{em}}_{-b,\xi} \tag{30}$$

and

$$\boldsymbol{E}^{\mathrm{em}}_{0,\eta}=\begin{pmatrix} E^{\mathrm{em}+}_{0,\eta} \\ E^{\mathrm{em}-}_{0,\eta} \end{pmatrix}=\boldsymbol{T}(b)\ \ \boldsymbol{E}^{\mathrm{em}}_{-b,\eta} \tag{31}$$

with

$$\boldsymbol{T}(b)=\boldsymbol{T}(\zeta)|_{\zeta=b} \tag{32}$$

and dielectric constants expressed in equation (4). In light of Good and Karali's theory [7], the waves expressed as the left-hand sides of equations (30) and

(31) are actually for $z=0^+$, i.e. outside the chiral-nematic film in an isotropic medium. Since $\boldsymbol{E}^{\mathrm{em}}_{-b,\xi}$ and $\boldsymbol{E}^{\mathrm{em}}_{-b,\eta}$ are incoherent, the transmitted intensities can be expressed as follows:

$$I_0^{\mathrm{em}+} \propto |E_{0,\xi}^{\mathrm{em}+}|^2 + |E_{0,\eta}^{\mathrm{em}+}|^2 \tag{33}$$

and

$$I_0^{\mathrm{em}-} \propto |E_{0,\xi}^{\mathrm{em}-}|^2 + |E_{0,\eta}^{\mathrm{em}-}|^2. \tag{34}$$

For a film with thickness τ, the transmitted intensities at $z=0^+$ are

$$I_{\mathrm{R}} \propto \sum_{z=-\tau}^{z=0} I_0^{\mathrm{em}+} \propto \sum_{z=-\tau}^{z=0} (|E_{0,\xi}^{\mathrm{em}+}|^2 + |E_{0,\eta}^{\mathrm{em}+}|^2) \tag{35}$$

and

$$I_{\mathrm{L}} \propto \sum_{z=-\tau}^{z=0} I_0^{\mathrm{em}-} \propto \sum_{z=-\tau}^{z=0} (|E_{0,\xi}^{\mathrm{em}-}|^2 + |E_{0,\eta}^{\mathrm{em}-}|^2) \tag{36}$$

and the dissymmetry factor g_{e} is calculated by inserting equations (35) and (36) into equation (1). Note that equations (33)–(34) are characterized by a single proportionality constant because of the isotropic environment where $z=0^+$ is located.

In the implementation of the CPF theory, an excitation beam of a polarization state defined by equation (8), such as linear and circular polarization, can be employed. In the present theoretical and experimental treatments of CPF, both left- and right-handed circularly polarized excitations were considered.

3. Experimental

A room temperature, chiral nematic liquid crystal host in a left-handed helical arrangement was formulated by mixing a nematic liquid crystal, BDH 18523 (m.p. = 2°C, $n=1{\cdot}4949$, $\Delta n=0{\cdot}0506$ at 436 nm, Merck), with cholesteryl oleate (99 per cent, m.p. = 44–47°C, Janssen Chimica). A fluorescent dye, 1,6-diphenylhexatriene (DPH) (>99 per cent, Fluka), was doped into the host at a level of 0·005 mol l^{-1}. The native pitch length, p, was measured from the Grandjean–Cano steps formed in a wedge [12], and p^{-1} was found to be proportional to the amount of cholesteryl oleate with a proportionality constant of 0·0482 μm^{-1} wt $\%^{-1}$. The centre wavelength of the selective reflection band was then calculated using a well-established equation, $\lambda_{\mathrm{R}}=np$. Since cholesteryl oleate has an average index of refraction around 1·50 [13], the n value of its binary mixture with BDH 18523 up to 10 wt % should remain practically constant at 1·50. The twisted nematic cell was fabricated by filling the CLC material between two fused silica substrates, which were coated with Nylon 66 as an alignment layer. The thickness of the cell was 11 μm. The directions of buffing on the two substrates were adjusted to fit the native pitch length.

A spectrofluorimeter (MPF-66, Perkin–Elmer), equipped with the optical system described in figure 3, was employed to measure CPF with left- and right-handed circularly polarized excitations. To minimize the optical loss due to reflection, an index matching fluid with $n=1{\cdot}500$ (Refractive Index Fluid, Cargille Laboratories Inc., NJ) was placed between the UG 11 band pass filter and the sample device. The circular polarizer, consisting of a linear polarizer and a quarter waveplate, was carefully balanced to ensure that there was no CPF from an isotropic fluorescent film. The fluorescence spectra were collected from an excitation wavelength of 350 nm. A typical set of fluorescence spectra is reproduced in figure 4. The emission intensities at 458 nm were employed for the calculation of g_{e} using equation (1). All measurements were carried out at 24·0 ± 0·2°C, and the reported g_{e} carries an experimental uncertainty as indicated by the error bars in figure 5.

To determine the second- and fourth-rank order parameters of DPH in the nematic host, BDH 18523, the linearly polarized emission, $I^{\mathrm{em}}_{\xi\xi}$ and $I^{\mathrm{em}}_{\xi\eta}$, $I^{\mathrm{em}}_{\eta\xi}$ and $I^{\mathrm{em}}_{\eta\eta}$, excited by a linearly polarized beam, I^{ex}_{ξ} and I^{ex}_{η}, respectively, were measured using the same setup for CPF with the same excitation wavelength. With the assumption that $\varphi=0$, the order parameters can be calculated [13] from emission anisotropies, defined as R_1 and R_2 below, using equations (37) and (38):

$$R_1 = \frac{I^{\mathrm{em}}_{\xi\xi} - I^{\mathrm{em}}_{\xi\eta}}{I^{\mathrm{em}}_{\xi\xi} + 2I^{\mathrm{em}}_{\xi\eta}} \tag{37}$$

and

$$R_2 = \frac{I^{\mathrm{em}}_{\eta\eta} - I^{\mathrm{em}}_{\eta\xi}}{I^{\mathrm{em}}_{\eta\eta} + 2I^{\mathrm{em}}_{\eta\xi}} \tag{38}$$

order parameters S_{em} and $\langle P_4\rangle_{\mathrm{em}}$ can be calculated [14] using equations (39) and (40):

$$S_{\mathrm{em}} = \frac{2 + 7R_1 - 14R_2 + 5R_1R_2}{23 - 14R_1 + R_2 - 10R_1R_2} \tag{39}$$

and

$$\langle P_4\rangle_{\mathrm{em}} = \frac{-12 + 21R_1 + 21R_2 - 30R_1R_2}{23 - 14R_1 + R_2 - 10R_1R_2}. \tag{40}$$

4. Results and discussion

To test the theory as presented above, we first carried out measurement and estimation of system parameters. Both BDH 18523 and cholesteryl oleate are transparent to the excitation wavelength of 350 nm. Therefore, order parameters, S_{ab}, S_{em}, and extinction coefficients, α_ξ, α_η, and α, all refer to the dopant molecules (i.e. DPH). Because of the low concentration of cholesteryl oleate in BDH 18523, the chiral nematic film is loosely pitched. Thus, the order parameter in the film was approximated

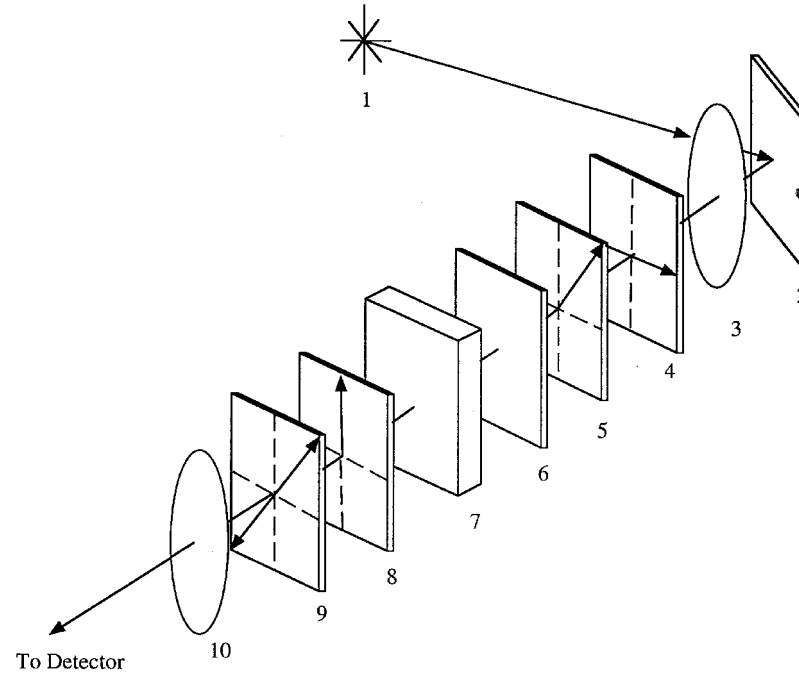

Figure 3. A schematic of the optical setup for the measurement of dissymmetry factor. Both excitation and emission beams are normal to the chiral nematic film. Linear polarizer 4 and quarter waveplate 5 form the excitation circular polarizer. Quarter waveplate 8 and linear polarizer 9 form the emission circular polarizer. Linear polarizer 9 is aligned at 45° to the horizontal to eliminate instrumental polarization. Handedness of circular polarization is reversed by rotating the quarter waveplate by 90°.

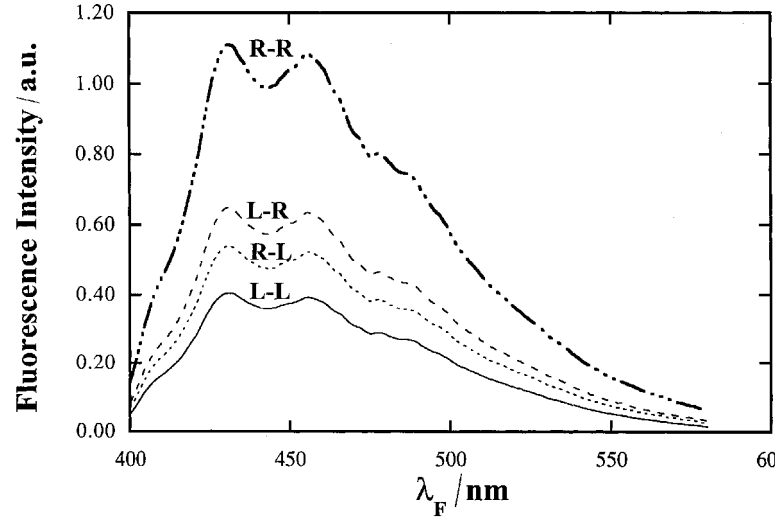

Figure 4. Fluorescence intensities of DPH, at an excitation wavelength of 350 nm, in a chiral nematic film consisting of BDH 18523 plus 1·5 wt % cholesteryl oleate with a native helical pitch length of 13·8 μm. R-L: RHCP excitation–LHCP detection; R-R: RHCP excitation–RHCP detection; L-L: LHCP excitation–LHCP detection; L-R: LHCP excitation–RHCP detection.

by that in the nematic film doped with DPH. Based on previous studies on DPH [2, 15], the emission dipoles are approximately parallel to its long molecular axis, namely $\varphi \approx 0$. The anisotropic molar extinction coefficient, α_ξ and α_η, at the excitation wavelength of 350 nm were determined to be $1{\cdot}084 \times 10^5$ and $2{\cdot}025 \times 10^4$ l mol^{-1} cm^{-1}, respectively, from which both $S_{ab} = 0{\cdot}59$ and $\alpha = 4{\cdot}963 \times 10^4$ l mol^{-1} cm^{-1} were found using equation (18). The emission anisotropies, R_1 and R_2, at 458 nm were determined to be 0·525 and $-0{\cdot}306$, respectively, with which order parameters S_{em} and $\langle P_4 \rangle_{em}$ were found to be 0·54 and $-0{\cdot}15$, respectively. The value of S_{ab} is slightly higher than S_{em}, as has been observed previously [14, 16]. In our theoretical treatment, S_{ab}, S_{em} and $\langle P_4 \rangle_{em}$ determined with linear dichroism and LPF from a nematic film were employed for the prediction of CPF from a series of chiral nematic films. In other words, all the parameters involved in the theory of CPF were independently determined for predictive purposes.

A total of eight devices, with a chiral concentration up to 10 wt % having a corresponding pitch length ranging from infinity to 2·07 μm, were used for the experimental characterization of CPF. The two emission peak wavelengths, 431 and 458 nm as shown in figure 4, were employed for the calculation of g_e. The resultant g_e as a function of λ_F^* with both left-handed circularly polarized (LHCP) and right-handed circularly polarized

(RHCP) excitations are displayed in figure 5. Theoretical predictions for the two excitation modes are also presented in figure 5 as two curves for a ready comparison with the experimental data. With all the system parameters determined *a priori*, the theory was found to be consistent with experimental observations, including the oscillatory character of the dependence of g_e on λ_F^*. Note that approximately the same degree of agreement between the theory and experiment was observed using emission peak intensities at 431 nm. The presently reported g_e values are at least twice as much as those observed by Stegemeyer *et al.* [2], although the polarization state of their excitation beam was not reported. One possible explanation for the enhanced g_e is that the alignment layer on the substrates minimizes defect formation. In fact, the g_e value in a device fabricated with substrates without alignment coating was found to diminish by half. In our experiment, the influence of the polarization state of the excitation beam was also considered.

Having gained our confidence in the theory, let us proceed to investigate the effects of dopant concentration, C, and film thickness using an LHCP excitation for illustrative purposes. Plotted in figure 6(*a*) are g_e as a function of λ_F^* at a series of DPH concentrations. It is clear that there is little effect presented by the doping level at $C \leqslant 0{\cdot}005\ \mathrm{mol\,l^{-1}}$, because the absorbance of excitation is so low that its intensity remains largely uniform throughout the entire film, as verified by the extinction coefficient of DPH at 458 nm, $\alpha = 4{\cdot}963 \times 10^4\ \mathrm{l\,mol^{-1}\,cm^{-1}}$. On the other hand, at a higher doping level, for example, $C = 0{\cdot}05\ \mathrm{mol\,l^{-1}}$, the penetration of the excitation into the film was found to be roughly half way into the film, and thus the other half of the film acts as a more efficient circular polarizer of the fluorescent beam, as demonstrated by a greater $|g_e|$ value. The effect of film thickness on g_e is revealed in figure 6(*b*). A low $|g_e|$ value is expected in a thin film, for example, 2 μm, in view of the diminished CP action furnished by the chiral nematic film. With an increasing film thickness, the maximum achievable g_e traverses a maximum, a theoretical prediction yet to be experimentally validated for rationalization.

5. Summary

In the absence of an overlap between absorption and emission, a theory was formulated for the photo-excited emission of chromophores from within a chiral nematic film in the spectral region outside the selective wavelength band. Salient features of the theory include: (1) the excitation beam undergoes circular dichroism (CD) and circular polarization (CP) while propagating through the film; (2) linearly polarized fluorescence occurs locally from nematic layers comprising the chiral nematic film; and (3) CP of the emitted beam while propagating through the rest of the film. With all the system parameters determined *a priori*, the predicted dissymmetry factor (g_e) was found to compare favourably with experimental observation at room temperature on 1,6-diphenylhexatriene doped into a chiral nematic fluid film consisting of BDH 18523 and cholesteryl oleate. The theory was thoroughly tested with two modes of excitation: left- and right-handed circular polarization. The theory was then employed to reveal the effects of several system parameters. It was found that (1) the concentration of the fluorescent dye in the chiral nematic film plays a role in affecting the g_e value; and (2) the maximum achievable g_e traverses a maximum at an increasing film thickness. Finally, we note that since fluorescent intensities resulting from LHCP and RHCP excitations are accessible through both theory and experimentation, it is possible to evaluate the dissymmetry factor achievable with an unpolarized excitation provided that

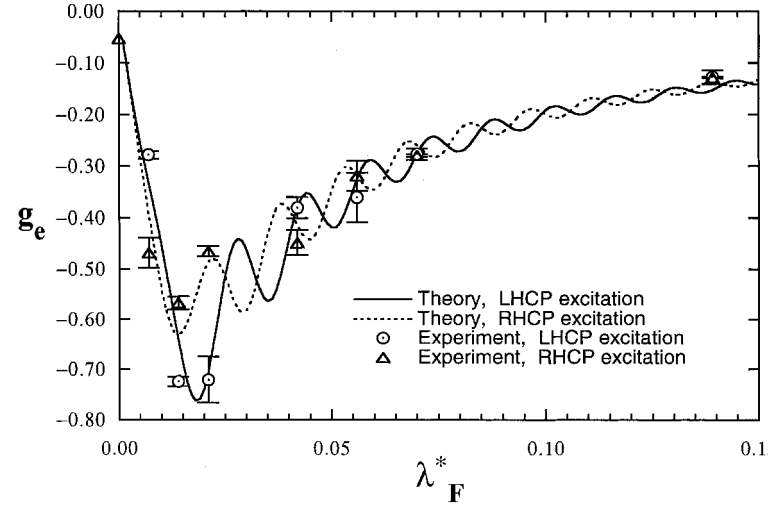

Figure 5. Experimentally observed g_e, based on the emission intensities at 458 nm, compared to theoretical prediction with two excitation modes: LHCP and RHCP. Parameters used in the prediction: $S_{ab} = 0{\cdot}59$, $S_{em} = 0{\cdot}54$, $\langle P_4 \rangle_{em} = -0{\cdot}15$, $\varphi = 0$, $n = 1{\cdot}50$, $\delta = 0{\cdot}0338$, $\alpha = 4{\cdot}963 \times 10^4\ \mathrm{l\,mol^{-1}\,cm^{-1}}$, film thickness = 11 μm, concentration of DPH $C = 0{\cdot}005\ \mathrm{mol\,l^{-1}}$. Note that the point at $\lambda_F^* = 0$ is for nematic film in which $\lambda_R \to \infty$.

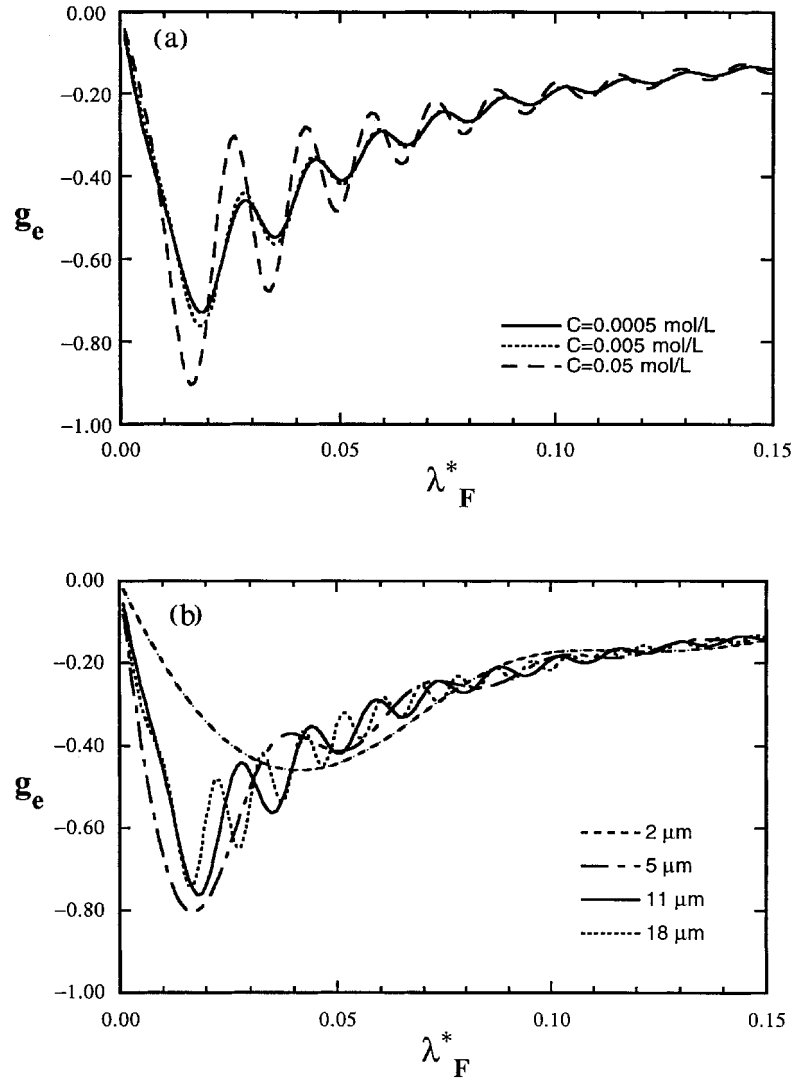

Figure 6. Theoretical prediction of g_e with LHCP excitation and the same parameter values as those used in figure 5 unless noted otherwise: (*a*) Effect of *C*, the concentration of DPH, on g_e; (*b*) Effect of film thickness on g_e.

incoherence and the random nature of an unpolarized light source can be ensured.

The authors wish to thank Professor Tetsuo Tsutsui of Kyushu University in Japan and Dr Ansgar Schmid of the Laboratory for Laser Energetics (LLE) at the University of Rochester for their advice and helpful discussion. They also thank Dr Stephen D. Jacobs of LLE for his suggestion of the optical system depicted in figure 3 for the characterization of CPF. This research was supported by US National Science Foundation under Grant CTS-9500737 and the Japanese Ministry of International Trade and Industry. Our advanced organic materials research was also supported in part by the US Department of Energy Office of Inertial Confinement Fusion under Cooperative Agreement No. DE-FC03-92SF19460, the University of Rochester, and the New York State Energy Research and Development Authority.

References

[1] Sackmann, E., and Voss, J., 1972, *Chem. Phys. Lett.*, **14,** 528.

[2] Stegemeyer, H., Stille, W., and Pollmann, P., 1979, *Israel J. Chem.*, **18,** 312.

[3] Pollmann, P., Mainusch, K.-J., and Stegemeyer, H., 1976, *Z. phys. Chem.*, **103,** 295.

[4] Sisido, M., Wang, X.-F., Kawaguchi, K., and Imanishi, Y., 1988, *J. phys. Chem.*, **92,** 4801.

[5] Kawaguchi, K., Sisido, M., and Imanishi, Y., 1988, *J. phys. Chem.*, **92,** 4806.

[6] Sisido, M., Takeuchi, K., and Imanishi, Y., 1984, *J. phys. Chem.*, **88,** 2893.

[7] Good, Jr, R. H., and Karali, A., 1994, *J. Opt. Soc. Am. A*, **11,** 2145.

[8] Belyakov, V. A., 1992, *Diffraction Optics of Complex-Structured Periodic Media* (New York: Springer), p. 105.

[9] SALEH, B. A., and TEICH, M. R., 1991, *Fundamentals of Photonics* (New York: Wiley), p. 171.
[10] BIRKS, J. B., 1970. *Photophysics of Aromatic Compounds* (New York: Wiley-Interscience), pp. 49, 51, 87.
[11] KASSUBECK, G., and MEIER, G., 1969, *Mol. Cryst. liq. Cryst.*, **8,** 305.
[12] SOMASHEKAR, R., and MADHAVA, M. S., 1987, *Mol. Cryst. liq. Cryst.*, **147,** 79.
[13] WOLARZ, E., and BAUMAN, D., 1991, *Mol. Cryst. liq. Cryst.*, **197,** 1.
[14] LAKOWICZ, J. R., 1983, *Principles of Fluorescence Spectroscopy* (New York: Plenum Press), p. 116.
[15] WOLARZ, E., and BAUMAN, D., 1995, *Liq. Cryst.*, **19,** 221.